BIOCHEMISTRY
including biophysical chemistry & molecular biology

Article

pubs.acs.org/biochemistry

Energetic and Structural Basis for Activation of the Epithelial Sodium Channel by Matriptase

Pradeep Kota,[†,‡,§] Agustin García-Caballero,[⊥,@] Hong Dang,[⊥] Martina Gentzsch,[⊥,∥] M. Jackson Stutts,*[,⊥] and Nikolay V. Dokholyan*[,†,‡,§,⊥]

[†]Program in Cellular and Molecular Biophysics, [‡]Center for Computational and Systems Biology, [§]Department of Biochemistry and Biophysics, and [∥]Department of Cell and Developmental Biology, University of North Carolina at Chapel Hill, Chapel Hill, North Carolina 27599-7260, United States

[⊥]Cystic Fibrosis/Pulmonary Research and Treatment Center, University of North Carolina at Chapel Hill, Chapel Hill, North Carolina 27599-7260, United States

Supporting Information

ABSTRACT: Limited proteolysis, accomplished by endopeptidases, is a ubiquitous phenomenon underlying the regulation and activation of many enzymes, receptors, and other proteins synthesized as inactive precursors. Serine proteases make up one of the largest and most conserved families of endopeptidases involved in diverse cellular activities, including wound healing, blood coagulation, and immune responses. Heteromeric α,β,γ-epithelial sodium channels (ENaC) associated with diseases like cystic fibrosis and Liddle's syndrome are irreversibly stimulated by membrane-anchored proteases (MAPs) and furin-like convertases. Matriptase/channel activating protease-3 (CAP3) is one of the several MAPs that potently activate ENaC. Despite identification of protease cleavage sites, the basis for the enhanced susceptibility of α- and γ-ENaC to proteases remains elusive. Here, we elucidate the energetic and structural bases for activation of ENaC by CAP3. We find a region near the γ-ENaC furin site that has previously not been identified as a critical cleavage site for CAP3-mediated stimulation. We also report that CAP3 mediates cleavage of ENaC at basic residues downstream of the furin site. Our results indicate that surface proteases alone are sufficient to fully activate uncleaved ENaC and explain how ENaC in epithelia expressing surface-active proteases can appear refractory to soluble proteases. Our results support a model in which proteases prime ENaC for activation by cleaving at the furin site, and cleavage at downstream sites is accomplished by membrane surface proteases or extracellular soluble proteases. On the basis of our results, we propose a dynamics-driven "anglerfish" mechanism that explains less stringent sequence requirements for substrate recognition and cleavage by matriptase than by furin.

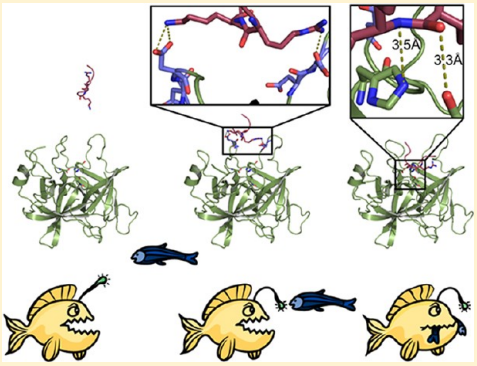

Limited proteolysis is the last step in the attainment of a functional form of many proteins of biological significance and perhaps the first step in protein degradation.[1] This important regulatory phenomenon is frequently observed in activation of many enzymes, hormones, receptors, and other biologically active proteins and is conserved through evolution.[2] Early structural studies of limited proteolysis led to two opposing theories that argued whether it is segmental mobility or surface accessibility of the proteolytic fragment that determines protease susceptibility.[3,4] Following these hypotheses, others have performed systematic computational analyses, concluding that local unfolding, in addition to segmental mobility and surface accessibility, guides protease susceptibility.[5,6] Although the structural requirements for cleavage by serine proteases are relatively well characterized,[7] the energetics of enzyme−substrate interactions remain unclear. Determining the energetics of enzyme−substrate interactions is critical to understanding the subtle differences in substrate specificities featured by serine proteases. The ENaC family of ion channels offers a unique platform for studying limited proteolysis because of the uniqueness of the mode of their regulation via cleavage by proteases, resulting in constitutive channel activation.

The epithelial sodium channel (ENaC) is considered the rate-limiting step in electrogenic absorption of Na^+ from luminal compartments lined by epithelia. Absorption of Na^+ by ENaC is critical in many biological processes, including renal and intestinal control of salt balance and blood pressure, and affects the functioning of many organs, including airways, sweat ducts, cornea, and inner ear.[8−11] Over the past decade, it has become clear that an important determinant of ENaC activity is the extent of partial proteolysis of the channel subunits.[12,13] Proteolytic regulation of ENaC includes selective cleavage by furin-like proteases during biosynthetic maturation as well as cleavage at the cell surface by proteases that can be membrane-associated or soluble. The current model of proteolytic

Received: September 21, 2011
Revised: March 26, 2012
Published: April 3, 2012

regulation of ENaC is that the open probability (P_O) of the heteromultimer is determined by cleavage events, so far confined to its α and γ subunits. In general, channels made of uncleaved subunits exhibit a very low P_O, and a range of cleavage events increases P_O. Two specific gaps in understanding proteolytic activation of ENaC involve the dominant role of γ-ENaC in proteolytic regulation of the channel. First, studies of at least five ENaC activating proteases identify essential sites in γ-ENaC, despite the accepted importance of furin-like cleavage sites in α-ENaC. Second, the structural and/or energetic features of the region of γ-ENaC (residues 130−200), which renders it susceptible to cleavage by multiple proteases, have not been investigated.

Previous studies of MAPs, including prostasin/CAP1 and TMPRSS4/CAP2, revealed an important role for γ-ENaC in channel regulation via limited proteolysis.[14−16] Additionally, the extracellular domain of γ-ENaC has been hypothesized to harbor an allosteric regulatory subdomain with an important role in channel function.[17] Interestingly, proteolytic activity of CAP1 is not required for its stimulation of ENaC. This observation led to a suggestion that CAP1 may play a critical noncatalytic role in ENaC regulation, perhaps as part of a cascade of surface-associated proteases.[18] It was recently demonstrated that matriptase/CAP3 is a critical activator of CAP1.[19] In this study, we focus on the activation of rat ENaC by CAP3-mediated cleavage of the γ subunit.

To uncover the energetic basis for activation of ENaC upon cleavage, we performed computational analyses on peptides from ENaC that are susceptible to proteolysis by serine proteases. We performed discrete molecular dynamics (DMD) simulations to elucidate the structural and energetic bases for ENaC peptide recognition by CAP3. Our computational studies of various peptide-binding configurations of CAP3 establish the structural and energetic bases for CAP3 activity. Using potential of mean force (PMF) analyses, we determined the energetic basis for substrate recognition and cleavage by CAP3. We compared the results to those obtained via similar analyses for furin and elucidated the energetic basis for the lower sequence specificity of CAP3 compared to that of furin. We designed experimental studies to identify CAP3-mediated cleavage sites in ENaC that lead to channel activation. We conclude that CAP3, with less stringent sequence requirements than furin, robustly activates ENaC by cleaving at multiple basic residues in the extracellular domain. Using computational and experimental studies, we show that a site upstream of the traditional furin site in γ-ENaC is a potential substrate for CAP3. On the basis of our findings, we propose an "anglerfish" mechanism driven by the dynamics of the enzyme whereby the peptide substrate interacts with and is stabilized by the loops enveloping the active site of the enzyme and is subsequently subject to proteolysis. This two-step mechanism underscores the importance of the energetic contribution of surface loops in serine proteases to their proteolytic activity. Furthermore, this mechanism provides a broad outlook for understanding stringency in sequence requirements for cleavage by serine proteases.

MATERIALS AND METHODS

Enzyme−Peptide Docking. We represented γ-ENaC cleavage sites tentatively identified by mutagenesis by 8-mer peptides with the putative wild-type P4−P1 cleavage sequence contained in the first four residues. We constructed three linear 8-mer peptides from rat γ-ENaC (Seq1, 135-RKRREAGS; Seq2, 178-RKRKISGK; Seq3, 132-KESRKRRE) such that the P1 site is between the fourth and fifth residues. We chose the initial configuration for the peptide by random placement at sites distant from the active site of either enzyme. We imposed two distance constraints, one between the ε-nitrogen atom (NE2) of the active site histidine and backbone amine of the P1′ site on the peptide and the other between the γ-oxygen atom (OG) of the active site serine and carbonyl oxygen of the P1 site, to draw the peptide close to the active pocket. To prevent bias of the configuration of the peptide in the active site of the enzyme, we placed the peptide at 10 different, randomly chosen starting positions and with different orientations with respect to one another (Figure S2A,B of the Supporting Information). We performed replica exchange DMD simulations of each such initial configuration with eight replicas in a temperature range of 0.35−0.75 reduced unit at increments of 0.035 unit (Figure S2C of the Supporting Information).[20] DMD uses the Medusa force field to treat interactions between atoms in the macromolecule.[21] We used EEF1, an implicit solvation model, to treat the solvation of the simulation system.[22] Energy minimization of the crystal structure of furin and matriptase was performed using Chiron prior to replica exchange simulations.[23] The total simulation time was 10^6 DMD time units for each replica. Each DMD time unit is approximately 50 fs in real time, accounting for a total simulation time of 50 ns per replica. The relationship between a DMD time unit and real time and their interconversion are discussed elsewhere.[24] Proteases were maintained static during simulations, allowing movement of only the loops surrounding the active site. We selected snapshots across simulation trajectories of all replicas that satisfied both the distance constraints and clustered them on the basis of the pairwise root-mean-square deviation (rmsd) of Cα atoms. We selected the representative structures from five such clusters and performed side chain optimization using the fixed backbone custom design protocol from the Medusa suite.[21]

PMF Calculations. To estimate the free energy of peptide binding for each enzyme−peptide combination, we computed two-dimensional (2D) PMF using the distance from the active site and energy as reaction coordinates. To obtain an accurate estimate of free energy, we removed the bias from the simulation trajectories by subtracting the appropriate value of constraint potential as a function of distance from the active site. We used the multiscale modeling tools for structural biology (MMTSB) toolkit[25] to perform WHAM (weighted histogram analysis method) analysis with replica exchange simulation trajectories and to compute PMFs at a given temperature. Using WHAM analysis, we self-consistently computed the density of states by combining overlapping histograms from different simulation trajectories.[26] We generated 2D contour plots of the 2D PMF values using gnuplot (http://www.gnuplot.info).

Peptide Disorder Prediction. We used Disopred2 (http://bioinf.cs.ucl.ac.uk/disopred) to analyze the peptide sequences of the α, β, and γ subunits of rat ENaC. We used residues L150−L290 from rat α-ENaC, K117−P240 from rat β-ENaC, and K91−S222 from rat γ-ENaC.

Plasmid Preparation. For biochemical analyses of ENaC subunit proteolysis, cDNAs encoding rat α-, β-, and γ-ENaC with HA-N-terminal (HA-NT) and V5-C-terminal (V5-CT) epitope tags were generated. Wild-type (WT) and mutant constructs (α-ENaC, R205A/R231A; β-ENaC and γ-ENaC, R135Q/K136Q/R137Q/R138Q, R135Q/K136Q/R137Q/

dx.doi.org/10.1021/bi2014773 | Biochemistry 2012, 51, 3460−3469

R138, R135Q/K136Q/R137/R138Q, R135Q/K136/R137Q/R138Q, and R135/K136Q/R137Q/R138Q), hepatocyte growth factor activator inhibitors 1 and 2 (HAI1 and HAI2, respectively), and CAP3 were generated by polymerase chain reaction and cloned into pCR-BluntII-TOPO (Invitrogen), linearized (*Hin*dIII), and transcribed in vitro using T7 RNA polymerase. A polyA tail was added after transcription (Ambion). Mutations were introduced with the Quikchange multi-site-directed mutagenesis kit (Stratagene). The WT ENaC plasmids were generously provided by B. Rossier. The sequences of all plasmids were verified at the University of North Carolina sequencing facility.

Western Blot Analysis. Proteins were extracted from oocytes as described above. Biotinylated and total proteins were solubilized by being boiled in Laemmli sample buffer for 10 min prior to being loaded onto 4 to 12% sodium dodecyl sulfate−polyacrylamide gel electrophoresis gels. Western blots were performed with anti-V5 (Invitrogen), anti-HA (Covance), anti-CAP3 (Bethyl Laboratories, Inc.), and anti-actin (Chemicon International) antibodies.

Functional Studies of ENaC in *Xenopus* Oocytes. V−VI stage healthy oocytes were harvested as described previously[27] and maintained in modified Barth's solution (MBS) at 18 °C. Animals were maintained and studied using protocols approved by the University of North Carolina Institutional Animal Care and Use Committee. Oocytes expressing the desired combinations of ENaC subunits and CAP3 were obtained as described previously.[14] Briefly, cRNAs encoding the WT of both untagged and HA-NT/V5-CT epitope-tagged subunits or mutant HA-NT/V5-CT-tagged subunits of rat α-, β-, and γ-ENaC (0.3 ng each) and CAP3 cRNA (typically 1 ng) were co-injected into oocytes. Twenty-four hours after injection, two-electrode voltage clamping was performed using a Genclamp amplifier (Axon Instruments) in a constant perfusion system. Currents were measured in the presence and absence of 10 μM amiloride, with the membrane voltage clamped to −100 mV. Currents were digitized and recorded using a Digidata 1200 A/D converter (Axon Instruments) and Axoscope software. After we had recorded the basal amiloride sensitive current (I_{Na}) by washing out amiloride, oocytes were superfused with amiloride-containing buffer and trypsin or hNE (2−20 μg/mL) for 5 min, followed by a second determination of I_{Na}. All results are expressed as means ± the standard error or as fold stimulation by CAP3 or hNE. The means of two groups were tested for significant differences using an unpaired Student's t test; differences among three or more groups were evaluated using analysis of variance (ANOVA) (GraphPad Prism). Proteins extracted from control and treated oocytes were analyzed by Western blots to verify expression of ENaC and actin.

Surface Labeling. *Xenopus* oocytes were treated with desired combinations of WT or mutant double epitope (HA/V5)-tagged rat ENaC α, β, and γ subunits (0.3 ng each) and with or without CAP3 cRNA (1 ng). After 24 h, 70 oocytes per experimental condition were prechilled on ice for 30 min and labeled with 0.7 mg/mL sulfo-NHS-biotin in MBS-Ca^{2+} buffer, 85 mM NaCl, 1 mM KCl, 2.4 mM $NaHCO_3$, 0.82 mM $MgSO_4$, 0.41 mM CaCl, 0.33 mM $Ca(NO_3)$, and 16.3 mM Hepes titrated to pH 8.0 with NaOH, while tumbling gently for 20 min at 4 °C. Oocytes were washed twice with chilled MBS-Ca^{2+} buffer and incubated in MBS-Ca^{2+} buffer with 100 mM glycine for 10 min at 4 °C to quench free biotin. Oocytes were washed again three times with chilled MBS-Ca^{2+} buffer and then lysed with lysis buffer [20 mM Tris, 50 mM NaCl, 50 mM NaF, 10 mM β-glycerophosphate, 5 mM $Na_4P_2O_7$ pyrophosphate, 1 mM EDTA (pH 7.5) containing protease inhibitors (complete, Roche), and aprotinin (Sigma)]. Cell lysates were prepared by passing oocytes through a 27G1/2 needle twice and by centrifugation at 3600 rpm for 10 min at 4 °C. Supernatants were transferred to new tubes, and samples were spun at 14000 rpm for 20 min at 4 °C. Supernatants were discarded and pellets solubilized in solubilization buffer [50 mM Tris, 100 mM NaCl, 1% Triton X-100, 1% NP-40, 0.2% SDS, 0.1% sodium deoxycholate, 20 mM NaF, 10 mM $Na_4P_2O_7$ pyrophosphate, 10 mM EDTA, and protease inhibitor cocktail (pH 7.5)]. Total inputs were taken from whole cell samples representing 4% of the total protein. Solubilized proteins were incubated with 100 μL of neutravidin beads (Pierce) overnight while tumbling at 4 °C. Samples were washed twice with 500 mM NaCl/50 mM Tris (pH 7.5) buffer and once with 150 mM NaCl/50 mM Tris (pH 7.5) buffer. Laemmli buffer was added, and samples were loaded on a 4 to 12% gradient Tris-glycine gel after incubation for 10 min at 96 °C. Samples were transferred to 0.45 μm polyvinylidene difluoride (PVDF) membranes (Millipore), and Western blot analysis was performed using anti-V5 (Invitrogen), anti-HA (Covance), and anti-actin (Chemicon International) monoclonal antibodies. Surface ENaC biotinylated fragments were quantified using the metamorph imaging 4.5 program (Hooker Microscopy Facility, University of North Carolina at Chapel Hill). Densitometry of selected bands was performed, using uninjected oocyte samples as the background signal.

RESULTS

CAP3 Has Less Stringent Sequence Requirements for Cleavage Than Furin. To assess the accessibility of the known protease cleavage tracts of different subunits of ENaC, we computed residue-wise disorder probability in the respective segments using Disopred2 (Figure S1 of the Supporting Information).[28] To eliminate any bias in the prediction, we considered segments (α, V151−L290; β, K117−P240; γ, K91−S222) such that most of the cleavage sites are enclosed but are not near either end of the segment. Interestingly, the regions susceptible to cleavage by furin-like convertases in the α and γ subunits (α, 202-RSSR, 228-RTAR; γ, 135-RKRR, 178-RKRK) of rat ENaC are intrinsically disordered (Figure S1A,C of the Supporting Information). The two peaks in the disorder plot for γ-ENaC correspond to the traditional furin site (135-RKRR-138) and the polybasic tract (178-RKRK-181) identified as cleavage sites for complete activation by furin and CAP1[16] (Figure S1C of the Supporting Information). This observation is in agreement with previous computational analyses reporting a preference for intrinsic structural disorder during cleavage by serine proteases.[5]

To elucidate the structural basis for substrate recognition and activation of ENaC by CAP3, we performed replica exchange DMD simulations[20,29] of three peptide sequences (Seq1, -2, and -3) from rat γ-ENaC (Materials and Methods) to study binding of the peptide to the active pocket of furin and CAP3 starting with the unbound state (Figure S2A,B of the Supporting Information). Using rmsd as the clustering criterion, we selected five final structures for each enzyme−substrate combination (Figure S2C of the Supporting Information). We found that the maximal rmsd between structures of peptide complexes with either furin or CAP3 is 1.5 Å. The final substrate-bound configurations of both furin and CAP3 satisfy the distance constraints imposed during

simulations (Materials and Methods and Figure 1A,C). The peptide-bound configurations also portray the differences in the

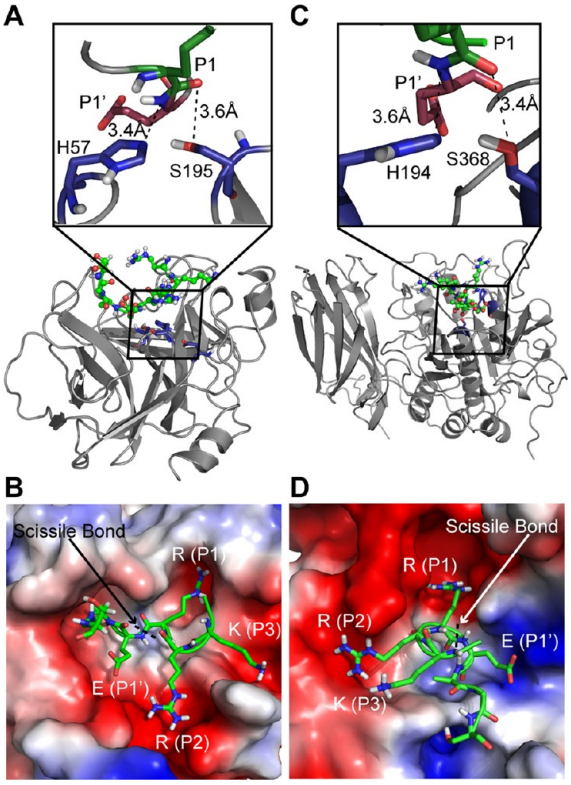

Figure 1. Structural models of peptides from γ-ENaC bound to furin and CAP3. (A) Final docked configuration of peptide Seq1 in the active pocket of CAP3. The inset shows the distances between the amine of the P1′ site from the NE2 group of the active site histidine and that of the carbonyl oxygen of the P1 site from the OG of the active site serine. (B) Electrostatic surface representation of CAP3 with the side chains of residues in peptide Seq1 shown as sticks. The guanidinium group of the arginine at the P1 site docks into a negatively charged groove in the enzyme. (C) Final docked configuration of peptide Seq1 in the active pocket of furin. The inset shows the distances between the amine of the P1′ site from the NE2 group of the active site histidine and that of the carbonyl oxygen of the P1 site from the OG site of the active site serine. (D) Electrostatic surface representation of furin with the side chains of residues in peptide Seq1 shown as sticks. The guanidinium group of arginine at the P1 site docks into a negatively charged groove in the enzyme.

size, shape, and charge distribution of the active sites of furin and CAP3 (Figure 1B,D). In our models, the residue at the P1 site of Seq1 is positioned in charge complementary pockets of both furin and CAP3 as observed in the corresponding crystal structures with bound inhibitors (Figure 1B,D).[30,31]

To establish the energetic basis for substrate recognition, we computed the 2D PMF with E (normalized energy) and d (distance in angstroms between active site residues and the P1 and P1′ sites on the peptide) as the two reaction coordinates. We have unbiased the constrained replica exchange simulations to obtain an accurate measure of the free energy of binding of the peptide to a given enzyme (Materials and Methods). We observe from the 2D-PMF contours that Seq1 features low-energy basins 3−5 Å from the active site of both CAP3 and furin (Figure 2A,B). Similarly, the polybasic tract consisting of the alternate furin cleavage site (178-RKRK) presents a low-energy basin ≤3−5 Å from the active site of both furin and CAP3, suggesting that binding of Seq2 to either enzyme is energetically favorable (Figure 2C,D, black arrows). Takeuchi et al. proposed that the lysine residue (K132) upstream of the traditional furin site could be the P4 site of a bona fide consensus cleavage motif (132-KESR) for CAP3.[32] To determine whether a peptide containing this amino acid sequence is energetically compatible to be in the vicinity of the active site of CAP3, we performed simulations with Seq3 approaching the active sites of CAP3 and furin. We observe low-energy configurations for Seq3 in the active site of CAP3 in simulations (Figure 2E and Movie 1 of the Supporting Information). Surprisingly, none of the configurations from the simulation with Seq3 in the presence of furin satisfied the distance constraints for recognition, suggesting that binding of Seq3 to furin is energetically less favorable (Figure 2F and Movie 2 of the Supporting Information). Such differences are reflected in the contour plot for furin and CAP3 with Seq3 where a low-energy basin 3−5 Å from the active site of furin is absent while a low-energy basin is observed in the case of CAP3 (compare panels E and F of Figure 2). These results indicate that CAP3 is more effective than furin at stimulating ENaC-containing γ-ENaC 132-KESR. Our computational results suggest low-stringency sequence requirements for CAP3-mediated cleavage and the presence of less ideal furin substrates in this region of γ-ENaC.

The Catalytic Activity of Matriptase Is Required for Activation of ENaC. To biochemically characterize the sequence requirements of CAP3, we first established that the catalytic activity of CAP3 is required for activation of ENaC. The motivation for this study arose from the fact that the catalytic activity of CAP1, a GPI-anchored membrane serine protease, is not required for its regulation of ENaC.[18] We found that coexpression of CAP3 with ENaC for 24 h robustly increased the basal amiloride sensitive sodium current (I_{Na}), typically in the range of 3−5-fold (Figure 3A). Moreover, unlike the basal I_{Na} generated by ENaC alone, the larger basal I_{Na} with CAP3 coexpression was not further increased by application of trypsin (Figure 3A) or hNE. The decrease in I_{Na} sometimes seen following exposure of CAP3-expressing oocytes to exogenous protease (Figure 3A, ENaC+CAP3, black bar) reflects run down of the stimulated I_{Na}. We observed that CAP3 stimulation of ENaC is inhibited by coexpressed hepatocyte activator inhibitor-1 (HAI-1) (Figure 3B). HAI-1 is a Kunitz-type serine protease inhibitor identified as the physiologic cognate inhibitor of CAP3 catalytic activity.[33] Western blots of CAP3 in lysates of the injected oocytes show that CAP3 was robustly expressed in its active form, as indicated by the expected fragmentation pattern of this self-activating protease (Figure 3C).[34] Furthermore, coexpression of HAI-1 with CAP3 prevented cleavage associated with CAP3 activation. Coexpression of HAI-2, a related Kunitz-type inhibitor, also completely prevented CAP3 stimulation of ENaC (Figure 3D).[35] Finally, CAP3 inactivated by mutation of S805 of the catlaytic triad had no effect on the I_{Na} of coexpressed ENaC (Figure 3D).[36] Thus, ENaC coexpressed with CAP3 is fully activated through a mechanism that requires the catalytic activity of CAP3.

CAP3 Cleaves γENaC at an Alternate Site N-Terminal to the Furin Site. We studied the role of γ-ENaC in stimulation by CAP3, by coexpressing the furin site mutants of α-ENaC with WT β- and γ-ENaC in oocytes. CAP3 robustly activated ENaC without the furin sites in the α-subunit,

dx.doi.org/10.1021/bi2014773 | Biochemistry 2012, 51, 3460−3469

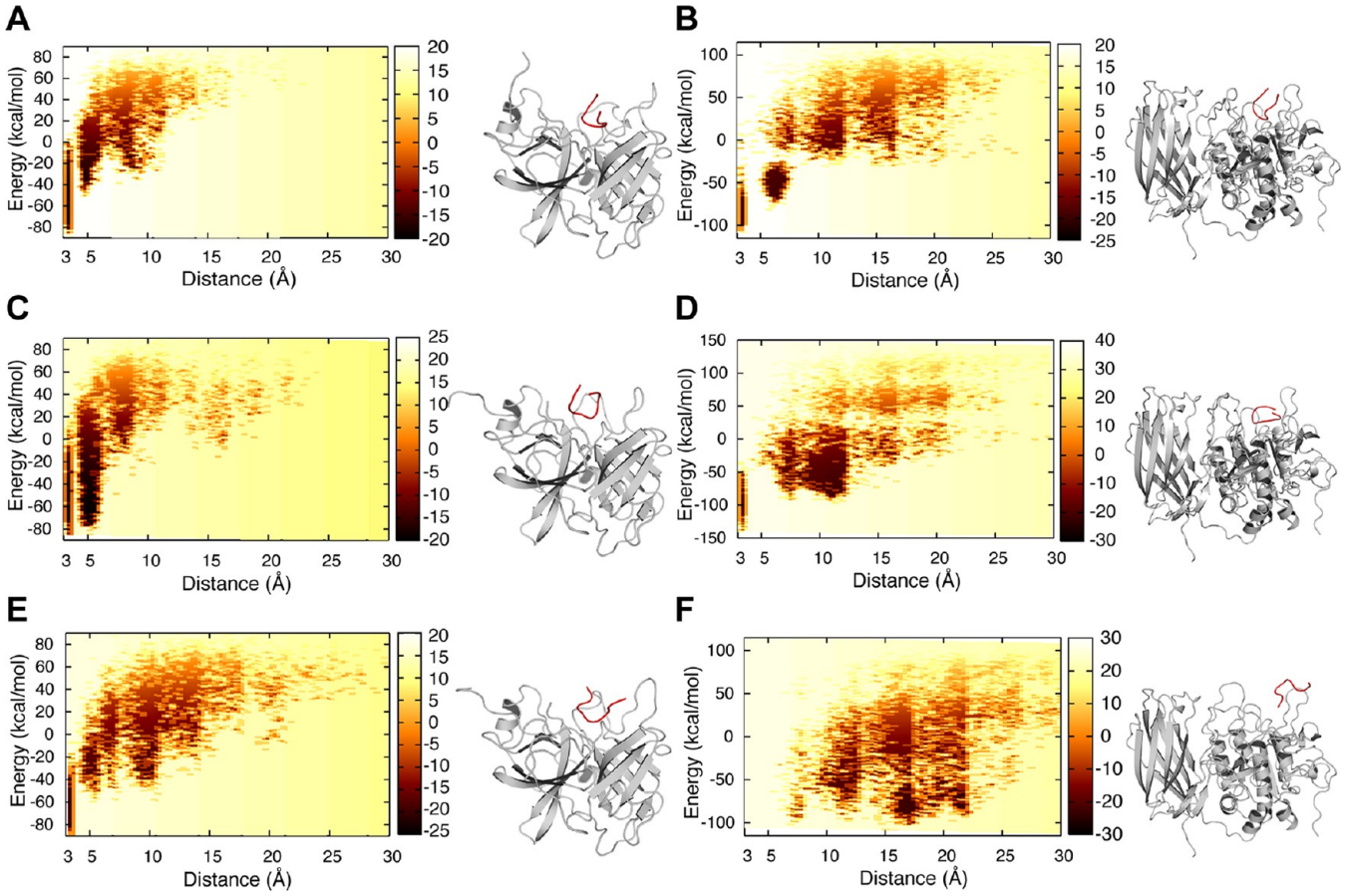

Figure 2. Energetic basis for binding of the peptide to furin and CAP3. 2D-PMF with a normalized energy of enzyme−substrate complex and distance between the active site and respective peptides as reaction coordinates. The color on the 2D-PMF plot is indicative of the free energy of binding of the peptide to the enzyme. The darker the color, the lower the free energy in kilocalories per mole. The peptide is colored red and the enzyme gray in the accompanying models representing the minimal energy configurations for the corresponding enzyme−peptide combinations. (A and B) 2D-PMF of binding of Seq1 to CAP3 and furin, respectively. (C and D) 2D-PMF of binding of Seq3 to CAP3 and furin, respectively. (E and F) 2D-PMF of binding of Seq3 to CAP3 (Movie 1 of the Supporting Information) and furin (Movie 2 of the Supporting Information), respectively. Seq3 is energetically incompatible to be in the vicinity of the active site of furin while it reaches the active site of CAP3.

suggesting predominant cleavage of the γ-subunit (Figure S3A,B of the Supporting Information). In γ-ENaC, we specifically examined the importance of the basic P1 residue (R138) in the 135-RKRR tract recognized as the furin site. Coexpressed CAP3 robustly stimulated ENaC containing γ subunit furin resistant mutant R138K and the CAP2 insenstive furin mutant R138A (Figure S3C,D of the Supporting Information),[14] indicating that CAP3 activates ENaC by a mechanism involving cleavage at a site distinct from γ-R138. Although the consensus sequences for convertases (R/K-X-X-R) and CAPs (R/K-X-X-R/K) overlap, some studies have reported distinct preferences at individual residue positions.[37,38] Therefore, we asked if extensive mutagenesis of the 135-RKRR tract in γ-ENaC to 135-QQQQ would affect the action of CAP3 toward ENaC. Coexpressed CAP3 did not stimulate this mutant ENaC, even though subsequent trypsin exposure led to significant stimulation (Figure 4B). Further mutagenesis revealed that the presence of R135 is sufficient for CAP3-mediated cleavage of γ-ENaC (Figure S4 of the Supporting Information).

To biochemically characterize CAP3-mediated cleavage of γ-ENaC, we performed Western blot analysis of a biotinylated surface protein pool captured on streptavidin beads (Materials and Methods). We characterized the HA/V5 double epitope-labeled γ-ENaC by the pattern of anti-V5 (C-terminal tag) and anti-HA (N-terminal tag) staining on the Western blot (Figure 4C). In oocytes expressing WT ENaC subunits, V5-tagged γ-ENaC at the cell surface exists as a mixture of full-length (FL, ∼93 kDa band) and furin fragments (FF, ∼75 kDa band) (Figure 4C, top panel). Under basal conditions, the HA label was found in a complementary ∼18 kDa band (Figure 4C, bottom panel) and in a FL band (not shown). With coexpression of CAP3, a more rapidly migrating fragment of ∼70 kDa (DF, distal fragment) replaces the FF band, a result now seen as being characteristic of proteolysis of γ-ENaC at a site 20−40 residues downstream of the furin site.[16,39,40] The 18 kDa anti-HA reactive (N-terminal) fragment indicates that cleavage at the traditional furin site is not affected. As predicted, mutant γ-ENaC containing the 135-QQQQ tract shows no FF, either V5- or HA-labeled, when coexpressed with α- and β-ENaC alone (Figure 4C, lane 4). However, when it is coexpressed with CAP3, the proportion of FL V5-labeled γ-135-QQQQ at the cell surface decreases, with a significant increase in the intensity of the DF fragment (Figure 4C, lane 5). A complementary N-terminal HA-labeled mutant γ-ENaC fragment of ∼23 kDa appears at the surface of CAP3-coexpressing cells (Figure 4C, bottom panel, lane 5). These results indicate that cleavage within the furin site of residues

dx.doi.org/10.1021/bi2014773 | *Biochemistry* 2012, 51, 3460−3469

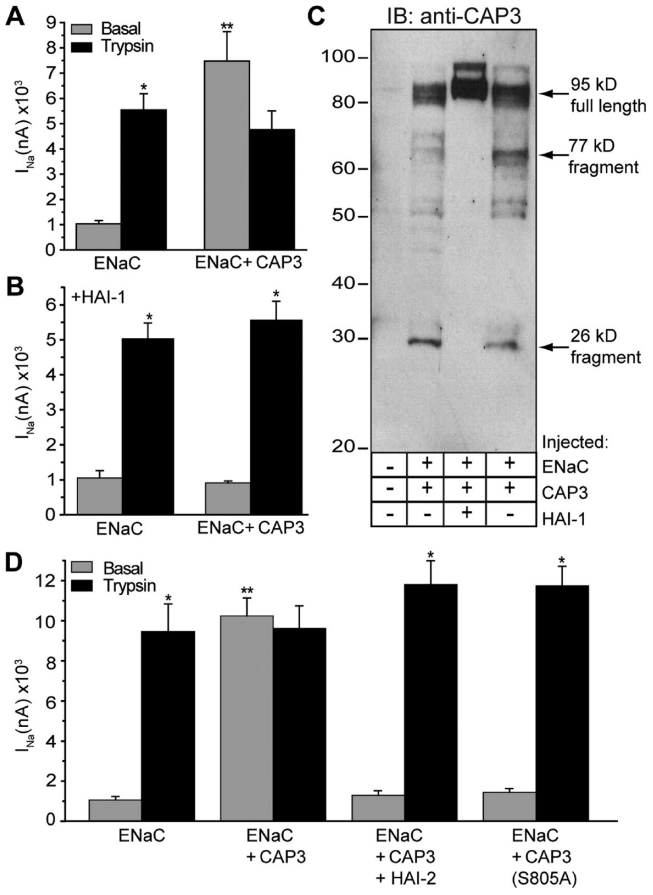

Figure 3. Catalytic activity of matriptase/CAP3 that is required for stimulation of ENaC. (A and B) Coexpression of the Kunitz domain-containing inhibitor, HAI-1, blocks stimulation of ENaC. Oocytes were co-injected with 0.3 ng of cRNA of α-, β-, and γ-ENaC alone (A) or in combination with 1 ng of cRNA of HAI-1 (B). After incubation for 24 h, the amiloride sensitive current (I_{Na}) was recorded before (gray bars) and after (black bars) a 5 min exposure to 2 μg/mL trypsin. (C) Expression and autocleavage of matriptase/CAP3 and effect of HAI-1. Oocyte lysates from panels A and B were studied by Western blotting using the anti-CAP3 antibody. (D) CAP3 stimulation of ENaC was blocked by coexpressed HAI-2 or by mutating serine 805 of the catalytic triad. Experiments were repeated on two to four batches of oocytes, with a total of 12−26 oocytes per condition. One asterisk indicates that the trypsin-stimulated I_{Na} is different from the basal I_{Na}. Two asterisks indicate that the basal I_{Na} is different from that of ENaC alone. Via ANOVA, $p < 0.05$.

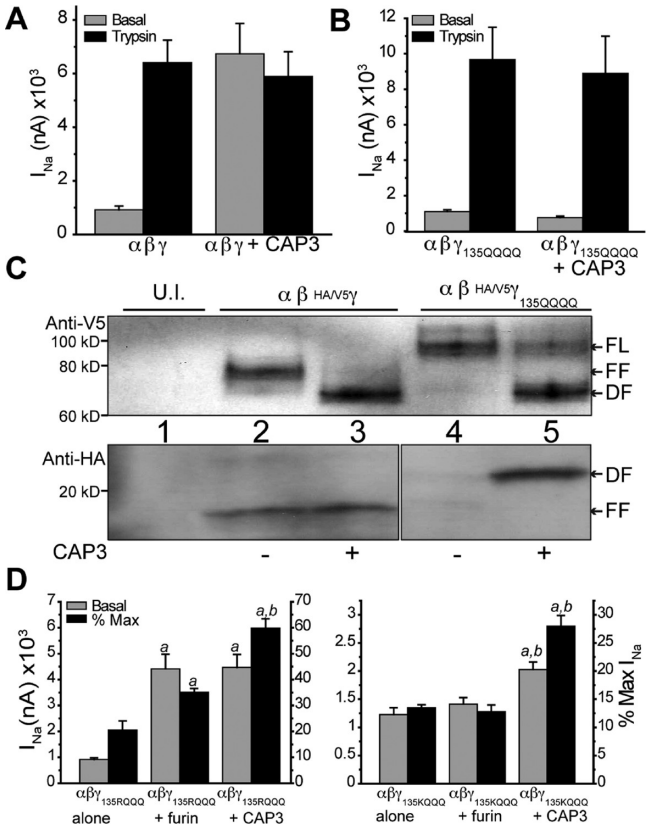

Figure 4. CAP3 mediates neither activation nor cleavage of γ-135-QQQQ ENaC. (A) WT ENaC was expressed alone or with CAP3. I_{Na} was recorded 24 h after cRNA injection, before (gray bars) and after (black bars) a 5 min trypsin exposure. (B) ENaC containing the γ-135-QQQQ mutant was expressed alone or with CAP3. I_{Na} was recorded as in panel A. (C) ENaC made of WT subunits or containing the mutant γ-135-QQQQ were expressed alone or with CAP3. After 24 h, uninjected (U.I.) oocytes and oocytes from each treatment group were biotinylated on their surface, and the surface protein pool was captured on streptavidin beads. Full-length HA/V5 γ-ENaC and fragments of HA/V5 γ-ENaC were recognized by blotting for V5 (C-terminal epitope) or HA (N-terminal epitope). Abbreviations: FL, full length; FF, furin fragment; DF, distal fragment. (D) Oocytes were treated with α_{FM}, β, and either γ-135-RQQQ (left) or γ-135-KQQQ (right). Each of these ENaC combinations was expressed alone or coexpressed with furin or CAP3 and studied after 24 h. The basal I_{Na} was recorded before and after a 5 min exposure to 2 μg/mL hNE. The basal I_{Na} as raw current (left ordinate) or as a percent of the maximal I_{Na} following elastase (right ordinate) is shown. Mean values were compared by ANOVA, and Tukey's test was applied. *a* denotes a value different from that of the γ mutant alone and *b* a value different from that of the γ mutant with furin ($p < 0.01$).

135−138 is blocked in γ-135-QQQQ, while CAP3 induces cleavage C-terminal to the furin site. In addition, we conclude that cleavage within residues 135−138 is essential for CAP3 stimulation of ENaC.

On the basis of previous reports and our computational analyses, we hypothesized that K132 could be part of a bona fide consensus motif (132-KESR) targeted by transmembrane serine proteases (TSPs) or furin-like convertases.[32,41] To test this hypothesis, we generated γ-ENaC with 132-HESRQQQ, which associates with WT α- and β-ENaC to produce a reduced I_{Na} that responds briskly to hNE (2 μg/mL) or trypsin (20 μg/mL) (Figure S4 of the Supporting Information, black bars). Although the presence of 132-KESR is evidently not optimal for endogenous convertases, we reasoned that overexpressed furin might recognize this site. Because the preference of furin at the P1 residue for arginine over lysine is strong,[42] while CAP3 is reported to tolerate lysine at P1,[32] we compared the ability of coexpressed human furin and CAP3 to stimulate the γ-ENaC mutants 135-RQQQ and 135-KQQQ. To simplify the interpretation, we expressed these mutant γ subunits with WT β-ENaC and the α-ENaC furin site mutant (Figure 4D). Interestingly, coexpressed human furin partially activated ENaC containing γ-132-KESRQQQ, to 35% of the maximal stimulated I_{Na}, albeit less efficiently than CAP3, which led to 60% of the maximal stimulated I_{Na} (Figure 4D, left panel). Coexpressed furin did not stimulate ENaC with a lysine at position 135 (Figure 4D, right panel), while CAP3 stimulated this mutant, albeit to a lesser extent than the mutant with R135 preserved. These results suggest that CAP3, because of its less

dx.doi.org/10.1021/bi2014773 | *Biochemistry* 2012, 51, 3460−3469

stringent sequence requirements, can target basic residues in the tract of residues 132−138 of γ-ENaC that are more resistant to endogenous convertases and overexpressed furin.

CAP3 Cleaves ENaC at Multiple Sites C-Terminal to the Furin Site. A candidate site for cleavage events responsible for the broadly staining DF (~70 kDa) (Figure 4C) is the 178-RKRK tract, as this polybasic region is required for cleavage of γ-ENaC by CAP1[16] and shares the same minimal sequence requirements for cleavage with CAP3.[43] DMD simulations revealed that binding of CAP3 or furin at this site is energetically favorable. Surprisingly, however, γ-ENaC with 178-QQQQ was stimulated by coexpressed CAP3 to approximately the same extent as ENaC containing the WT γ subunit (Figure 5A). The CAP3-stimulated basal current in

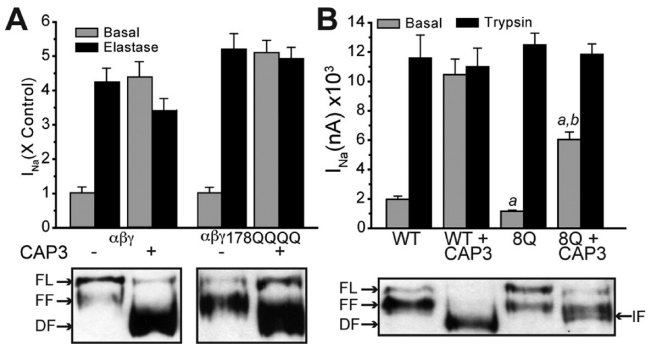

Figure 5. Basic tract 178-RKRK in γ-ENaC is not essential for CAP3 stimulation of I_{Na}. (A) WT HA/V5 γ-ENaC or HA/V5 γ-RKRK(178−181)QQQQ cRNA was co-injected with WT α- and β-ENaC cRNA (0.3 ng/subunit). Half of each group was also injected with 1 ng of cRNA for CAP3. I_{Na} was recorded after 24 h, before and after a 5 min exposure to 2 μg/mL hNE (top; N = 10−12 oocytes per condition from two batches). Thirty to sixty oocytes per condition were surface biotinylated, as described elsewhere. WT and mutant γ-ENaC fragments present in the cell surface pool were analyzed by a Western blot (bottom). (B) WT α- and β-ENaC subunits were expressed for 24 h with WT or mutant (8Q) HA/V5 γ-ENaC, with or without CAP3 (see the text for a description of mutant 8Q). I_{Na} was recorded before and after a 5 min exposure to 20 μg/mL trypsin [*a* denotes a value different from the WT basal value and *b* a value different from the 8Q basal value (p < 0.01)] Surface-biotinylated proteins from the same injection groups analyzed by anti-V5 Western blotting are shown in the bottom panel. Abbreviations: FL, full-length; FF, furin fragment; DF, distal fragment; IF, intermediate fragment.

either WT or mutant channel groups was not further increased by hNE, indicating that CAP3 attained full proteolytic stimulation of mutant ENaC at the surface. In addition, the patterns of C-terminal V5-labeled fragments of WT or mutant γ-ENaC contained in the cell surface pool of each expression group were affected similarly by coexpressed CAP3, each showing a shift from a mixture of FL or FF to a population dominated by DFs, consistent with CAP3-induced cleavage at sites downstream from the furin site (Figure 5A, bottom panel). While these results do not refute the fact that the 178-RKRK tract is a potential cleavage site, the data indicate that other potential cleavage sites exist in the vicinity of this basic tract.

As mutation of the 178-RKRK polybasic tract has no effect on CAP3-mediated stimulation or the banding pattern of γ-ENaC fragments, we tested the contribution of flanking basic residues in the region from residue 172 to 202. We investigated the importance of 172R, 185K, 189K, 201K, and 202K, individually and in various combinations with the 178-QQQQ tract. We observed no significant effects of mutating any single basic residue in this region on CAP3 cleavage and stimulation of ENaC. However, from a threshold of mutating six or seven basic residues, up to nine basic residues in this region replaced with glutamine, we observed progressively decreased CAP3-mediated stimulation of I_{Na}, staining density of DF, and resting whole cell P_O. In particular, ENaC containing mutant γ subunits with eight glutamines substituted for basic residues within the tract of residues 172−202 (8Q) was only partially stimulated by coexpressed CAP3 (Figure 5B). Western blot analysis of the C-terminal V5-tagged fragments of 8Q γ-ENaC on the cell surface suggests that in this extensively mutated channel, CAP3 generates an intermediate fragment (IF) that migrates between FF and DF, characteristic of WT γ-ENaC (Figure 5B). Thus, CAP3 cleaves ENaC at multiple basic sites, including those that do not conform to the furin consensus sequence requirements. These results are in agreement with our conclusion that CAP3 has less stringent sequence requirements for cleavage than furin. It is likely that the local structure of the protein is altered upon extensive mutagenesis, thereby hampering cleavage. Assuming that the structure of ENaC is intact, our results suggest that CAP3 cleaves γ-ENaC at multiple sites C-terminal to the furin site, resulting in robust channel activation.

DISCUSSION

Here, we report the energetic, structural, and sequence requirements for cleavage of ENaC by CAP3 and furin. While we focus our attention on activation of ENaC by proteases, the results of our computational analyses can be broadly applied to catalysis by serine proteases. Limited endoproteolysis of ENaC is a complex mechanism for regulating absorption of Na^+ by epithelia. Numerous proteases that stimulate ENaC have been identified, alongside endogenous protease inhibitors that oppose this effect.[12,13] Thus, ENaC may be controlled in a tissue specific manner by the complement of endogenous proteases and anti-proteinases expressed in a given cell type. We experimentally characterized the effects of CAP3 coexpression on proteolysis and stimulation of ENaC in *Xenopus* oocytes. We identified two regions of γ-ENaC susceptible to direct cleavage by CAP3. Cleavage after any of several basic residues within each region is necessary and sufficient for full stimulation of ENaC. These observations support three main conclusions. First, cleavage of the γ subunit alone accounts for CAP3 stimulation of ENaC. Second, though limited in extent, the specificity of γ-ENaC cleavage is not based on stringent docking of extended segments of γ-ENaC within the active site in CAP3. Instead, multiple basic residues comprising the γ-ENaC furin site, along with those including and flanking the 178-RKRK tract, are exposed for proteolysis. Finally, CAP3 alone can achieve full proteolytic stimulation of ENaC.

Structural studies of ENaC are set back because of the unavailability of a complete atomistic structure of the heteromultimer. Recently, different ENaC subunits were threaded onto the structure of a homologous acid-sensing ion channel (ASIC1).[44,45] In the sequence alignment used for model building, the region in γ-ENaC containing the putative cleavage sites for CAP3 and furin was designated the "hypervariable region".[44] Consequently, the structural features of this region are unavailable despite the modeling efforts. The observation that the protease cleavage sites in ENaC are intrinsically disordered is in line with the proposed structural requirement for serine protease activity.[5,6] To study the

dx.doi.org/10.1021/bi2014773 | *Biochemistry* 2012, 51, 3460−3469

energetic basis for substrate recognition by CAP3 and furin, we performed DMD simulations of both enzymes with different candidate peptides. Although crystal structures of matriptase/CAP3 [Protein Data Bank (PDB) entry 1EAW] and furin (PDB entry 1P8J) with bound inhibitors are available for this effort,[30,31,46] we reasoned that the static orientation of an inhibitor in the catalytic pocket does not effectively capture the dynamics of enzyme−substrate complexes. Therefore, we resorted to DMD simulations, and we observed from the low-energy configurations that a charge complementary pocket in both furin and CAP3 mediates critical enzyme−peptide interactions (Figure 1B,D). While these simulations are not intended to model the hydrolysis reaction conducted by either enzyme, they provide insight into the binding properties of a given enzyme−peptide combination. Given that substrate recognition is the first step in hydrolysis, we consider a peptide that can reach the vicinity of the enzyme (3−5 Å) as a potential substrate for cleavage. By keeping most of the enzyme static during simulations, we assume that furin and matriptase do not undergo significant conformational changes during peptide recognition. Furthermore, by using an implicit solvent model (EEF1) for treating solvent interactions, we disregard specific water-mediated hydrogen bond formation involved in hydrolysis. Therefore, our simulation studies are aimed at determining only whether a given peptide is energetically suitable for presenting itself in the proximity (within 3−5 Å) of the active site of furin or matriptase and not to quantify the rate of hydrolysis of a given peptide by a protease. PMF analysis with Seq1 features low-energy basins at the active sites of both furin and CAP3, suggesting that Seq1 can be a substrate for both enzymes. Interestingly, an analogous computational study of Seq3 indicates that the 132-KESR tract can be a substrate for CAP3 but not for furin. This result is consistent with our observation that CAP3 cleaves and stimulates ENaC effectively when 132-KESR are the only potentially susceptible residues available near the furin site, whereas exogenous furin is much less effective at stimulating ENaC in this context (Figure 3D). These computational analyses of WT sequences, with our functional and biochemical analyses of WT and mutant γ-ENaC, clearly indicate that the γ-ENaC sequence 132-KESRKRR is highly susceptible to cleavage by CAP3.

CAP3, unlike furin in this study, or CAP2 in our previous work,[14] appears to cleave γ-ENaC after several basic residues within the 132-KESRKRR tract, including 135R, 136K, and 138R. Such greater susceptibility of γ-ENaC to cleavage may reflect CAP3's low substrate stringency coupled with favorable substrate access due to local structural disorder. 2D PMF analyses of all peptide−catalytic site combinations considered in this study broadly support this notion. Energy minima at 3−5 Å indicate close contact between the peptide and catalytic site required for proteolysis (Figure 2), whereas low-energy basins beyond 5 Å are suggestive of electrostatic attraction between the net positively charged peptides and the negatively charged surface loops of the enzyme. The absence of a low-energy basin 3−5 Å from the active site reflects the fact that Seq3 is a less suitable substrate for furin than CAP3 (Figure 2E,F). Seq1 and Seq2 feature energy minima 3−5 Å from the active site of both CAP3 and furin (compare panels A and B and panels C and D of Figure 2). Low-energy basins corresponding to interaction between the peptide and the surface loops of the enzyme are observed beyond 5 Å for all peptides in simulations. However, only Seq1 and Seq2 are energetically compatible to be in the proximity of the active site of CAP3 and furin, as evidenced from the PMF analysis (Figure 2A−D). PMF analysis indicates that it is favorable for Seq3 to be in the vicinity of CAP3, but not furin. In light of these observations, we propose an anglerfish mechanism analogous to the characteristic mode of predation by the anglerfish where the fish represents the enzyme, with its illicium being the surface loops that capture the peptide to be cleaved and proteolysis being the eventual irreversible event (Figure 6). The realization of this mechanism

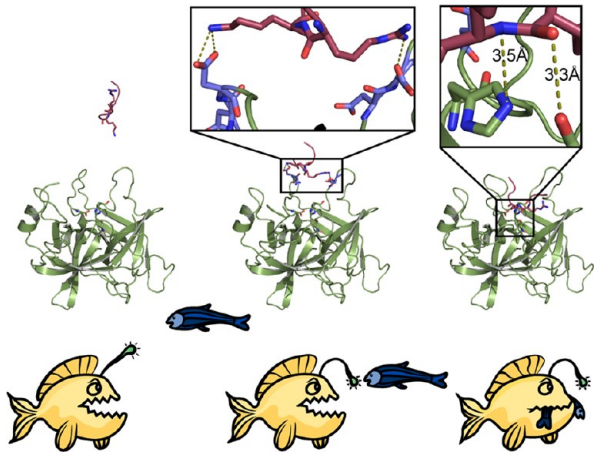

Figure 6. Anglerfish mechanism of peptide recognition and cleavage by MAPs. A two-step mechanism depicting the importance of surface loops in proteolysis by MAPs. The incoming peptide interacts with the surface loops and is ultimately delivered to the active site, resulting in irreversible cleavage. 2D PMF analyses reveal the energetic basis for this mechanism.

is confined by the assumption that proteolysis is guaranteed if a peptide is energetically compatible to be in the vicinity (3−5 Å) of the active site of a hydrolytic enzyme.

Our examination of CAP3 activity suggests that several different events underlie stimulation of ENaC. Mutational analysis suggests that 132K participates in a sequence (132-KESR) predicted to be optimal for cleavage by CAP3.[32] Residual cleavage and stimulation of ENaC containing γ-135-RQQQ requires the intact sequence 132-KESR. Mutagenesis of the furin sites in α-ENaC has no effect on CAP3 stimulation of ENaC, even though CAP3 converts all FL WT α-ENaC to fragments expected from cleavage at the two furin sites, similar to our previous study with CAP2.[14] The stimulation of ENaC by CAP1 was also linked by mutagenesis to γ-ENaC.[16] Complete proteolytic stimulation of ENaC by soluble serine proteases, including trypsin, hNE, and plasmin, is also exerted by cleavage of the γ subunit.[40,47,48] Thus, our results demonstrating that CAP3-mediated stimulation of ENaC can be blocked by mutations in γ-ENaC add to a growing body of data indicating that γ-ENaC plays a central role in the proteolytic regulation of ENaC.

On the basis of our results, cleavage of γ-ENaC mediated by CAP3 occurs in two regions. The first is discretely defined by the furin site, and the second includes basic residues centered on and surrounding the 178-RKRK tract. CAP3's low-stringency requirements for cleavage are consistent with its cleavage of γ-ENaC at multiple basic residues downstream of the furin cleavage site. Our results provide a compelling hypothesis that recognition and/or cleavage of γ-ENaC by proteases is substantially determined by the accessibility of key sites rather than solely by a stringent structural requirement.

dx.doi.org/10.1021/bi2014773 | *Biochemistry* 2012, 51, 3460−3469

The ability of certain proteases to activate ENaC has been linked to a specific residue or tract within the segment of residues 172−202.[16,40,47,48] On the basis of such work with prostasin (CAP1), the initial expectation was that CAP3 would cleave at the 178-RKRK tract. However, when the 178-RKRK tract is unavailable, both CAP2 and CAP3 readily cleave at multiple basic residues in the region of residues 172−202. This phenomenon is consistent with the concept that this region is highly accessible to proteases because of intrinsic structural disorder. The low stringency of CAP3 explains why we could not identify a single residue or short tract that can be mutated to block CAP3 stimulation of ENaC. We expect the accessibility of either region to increase with time and the extent of proteolysis, leading to further cleavage and consequent activation by relatively nonspecific proteases.

Our results indicate that CAP3 potently stimulates ENaC in an in vitro setting, which is dependent on direct catalytic attack of the protease on extracellular segments of γ-ENaC. It has been suggested that CAP3 completes its autoactivation at the cell surface.[49,50] As a step toward understanding the colocalization of ENaC and CAP3 in vivo, we performed immunofluorescence microscopy to confirm that matriptase localizes to the subapical pools near the plasma membrane of human bronchial epithelial (HBE) cells derived from different individuals (Figure S5 of the Supporting Information). ENaC can be detected in apical and subapical compartments of HBE cultures and is processed by limited cleavage in these cells.[51,52] Thus, it appears highly likely that ENaC is cleaved by matriptase in HBE cells. Additional work is needed to confirm that ENaC and active CAP3 occupy positions at the cell surface that allow ENaC cleavage, but our results clearly imply that CAP3 is capable of activating ENaC in a manner independent of furin-like convertases. CAP3 also activates CAP1,[53] which stimulates ENaC regardless of its catalytic activity.[54] These and other recent observations suggest a possibility for a cascade of interactions at the cell surface involving CAP3 and other proteases like CAP1, exercising dynamic control over proteolytic regulation of ENaC.[55]

We conclude that CAP3, a MAP, can independently activate ENaC without contributions from furin-like convertases or soluble proteases, without a requirement for specific structural motifs for recognition and/or cleavage. Our computational analyses give rise to a potentially generic anglerfish mechanism that can be broadly applied to serine protease-mediated recognition and cleavage.

■ ASSOCIATED CONTENT

Ⓢ Supporting Information

Figures supporting the results obtained in this study and movies representing computational trajectories. This material is available free of charge via the Internet at http://pubs.acs.org.

■ AUTHOR INFORMATION

Corresponding Author

*M.J.S.: e-mail, Jack_Stutts@med.unc.edu. N.V.D.: e-mail, dokh@unc.edu; phone, (919) 843-2513.

Present Address

[@]Hotchkiss Brain Institute, Calgary, AB, Canada.

Funding

This work was supported by National Institutes of Health Grants 5P01HL034322 and 5R01HL080561 (to M.J.S.) and R01GM080742 and ARRA Supplements GM080742-03S1 and GM066940-06S1 (to N.V.D.).

Notes

The authors declare no competing financial interest.

■ ACKNOWLEDGMENTS

We acknowledge the expert technical contributions of Yan Dang and Hong He. We thank Drs. Feng Ding and David Shirvanyants for helpful discussions on PMF calculations and data analysis.

■ REFERENCES

(1) Neurath, H., and Walsh, K. A. (1976) Role of proteolytic enzymes in biological regulation (a review). *Proc. Natl. Acad. Sci. U.S.A. 73*, 3825−3832.

(2) Neurath, H. (1984) Evolution of proteolytic enzymes. *Science 224*, 350−357.

(3) Neurath, H. (1989) Proteolytic processing and physiological regulation. *Trends Biochem. Sci. 14*, 268−271.

(4) Novotny, J., and Bruccoleri, R. E. (1987) Correlation among sites of limited proteolysis, enzyme accessibility and segmental mobility. *FEBS Lett. 211*, 185−189.

(5) Hubbard, S. J., Campbell, S. F., and Thornton, J. M. (1991) Molecular recognition. Conformational analysis of limited proteolytic sites and serine proteinase protein inhibitors. *J. Mol. Biol. 220*, 507−530.

(6) Hubbard, S. J., Beynon, R. J., and Thornton, J. M. (1998) Assessment of conformational parameters as predictors of limited proteolytic sites in native protein structures. *Protein Eng. 11*, 349−359.

(7) Perona, J. J., and Craik, C. S. (1995) Structural basis of substrate specificity in the serine proteases. *Protein Sci. 4*, 337−360.

(8) Kellenberger, S., Gautschi, I., and Schild, L. (2002) An external site controls closing of the epithelial Na^+ channel ENaC. *J. Physiol. (Oxford, U.K.) 543*, 413−424.

(9) Reddy, M., Wang, X., and Quinton, P. (2008) Effect of Cytosolic pH on Epithelial Na^+ Channel in Normal and Cystic Fibrosis Sweat Ducts. *J. Membr. Biol. 225*, 1−11.

(10) Kim, S. H., Kim, K. X., Raveendran, N. N., Wu, T., Pondugula, S. R., and Marcus, D. C. (2009) Regulation of ENaC-mediated sodium transport by glucocorticoids in Reissner's membrane epithelium. *Am. J. Physiol. 296*, C544−C557.

(11) Rauz, S., Walker, E. A., Murray, P. I., and Stewart, P. M. (2003) Expression and distribution of the serum and glucocorticoid regulated kinase and the epithelial sodium channel subunits in the human cornea. *Exp. Eye Res. 77*, 101−108.

(12) Rossier, B. C., and Stutts, M. J. (2009) Activation of the Epithelial Sodium Channel (ENaC) by Serine Proteases. *Annu. Rev. Physiol. 71*, 361−379.

(13) Kleyman, T. R., Carattino, M. D., and Hughey, R. P. (2009) ENaC at the Cutting Edge: Regulation of Epithelial Sodium Channels by Proteases. *J. Biol. Chem. 284*, 20447−20451.

(14) Garcia-Caballero, A., Dang, Y., He, H., and Stutts, M. J. (2008) ENaC Proteolytic Regulation by Channel-activating Protease 2. *J. Gen. Physiol. 132*, 521−535.

(15) Adachi, M., Kitamura, K., Miyoshi, T., Narikiyo, T., Iwashita, K., Shiraishi, N., Nonoguchi, H., and Tomita, K. (2001) Activation of Epithelial Sodium Channels by Prostasin in *Xenopus* Oocytes. *J. Am. Soc. Nephrol. 12*, 1114−1121.

(16) Bruns, J. B., Carattino, M. D., Sheng, S., Maarouf, A. B., Weisz, O. A., Pilewski, J. M., Hughey, R. P., and Kleyman, T. R. (2007) Epithelial Na^+ Channels Are Fully Activated by Furin- and Prostasin-dependent Release of an Inhibitory Peptide from the γ-Subunit. *J. Biol. Chem. 282*, 6153−6160.

(17) Winarski, K. L., Sheng, N., Chen, J., Kleyman, T. R., and Sheng, S. (2010) Extracellular allosteric regulatory subdomain within the γ subunit of the epithelial Na^+ channel. *J. Biol. Chem. 285*, 26088−26096.

(18) Vuagniaux, G., Vallet, V., Jaeger, N. F., Hummler, E., and Rossier, B. C. (2002) Synergistic activation of ENaC by three membrane-bound channel-activating serine proteases (mCAP1, mCAP2, and mCAP3) and serum- and glucocorticoid-regulated kinase (Sgk1) in *Xenopus* oocytes. *J. Gen. Physiol. 120*, 191−201.
(19) List, K., Hobson, J. P., Molinolo, A., and Bugge, T. H. (2007) Co-localization of the channel activating protease prostasin/(CAP1/PRSS8) with its candidate activator, matriptase. *J. Cell. Physiol. 213*, 237−245.
(20) Ding, F., Tsao, D., Nie, H., and Dokholyan, N. V. (2008) Ab initio folding of proteins with all-atom discrete molecular dynamics. *Structure 16*, 1010−1018.
(21) Ding, F., and Dokholyan, N. V. (2006) Emergence of protein fold families through rational design. *PLoS Comput. Biol. 2*, e85.
(22) Lazaridis, T., and Karplus, M. (1999) Effective energy function for proteins in solution. *Proteins 35*, 133−152.
(23) Ramachandran, S., Kota, P., Ding, F., and Dokholyan, N. V. (2011) Automated minimization of steric clashes in protein structures. *Proteins 79*, 261−270.
(24) Sharma, S., Ding, F., and Dokholyan, N. V. (2007) Multiscale modeling of nucleosome dynamics. *Biophys. J. 92*, 1457−1470.
(25) Feig, M., Karanicolas, J., and Brooks, C. L., III (2004) MMTSB Tool Set: Enhanced sampling and multiscale modeling methods for applications in structural biology. *J. Mol. Graphics Modell. 22*, 377−395.
(26) Kumar, S., Bouzida, D., Swendsen, R. H., Kollman, P. A., and Rosenberg, J. M. (1992) The weighted histogram analysis method for free-energy calculations of biomolecules. 1. The method. *J. Comput. Chem. 13*, 1011−1021.
(27) Donaldson, S. H., Hirsh, A., Li, D. C., Holloway, G., Chao, J., Boucher, R. C., and Gabriel, S. E. (2002) Regulation of the Epithelial Sodium Channel by Serine Proteases in Human Airways. *J. Biol. Chem. 277*, 8338−8345.
(28) Ward, J. J., Sodhi, J. S., McGuffin, L. J., Buxton, B. F., and Jones, D. T. (2004) Prediction and functional analysis of native disorder in proteins from the three kingdoms of life. *J. Mol. Biol. 337*, 635−645.
(29) Dokholyan, N. V., Buldyrev, S. V., Stanley, H. E., and Shakhnovich, E. I. (1998) Discrete molecular dynamics studies of the folding of a protein-like model. *Folding Des. 3*, 577−587.
(30) Henrich, S., Cameron, A., Bourenkov, G. P., Kiefersauer, R., Huber, R., Lindberg, I., Bode, W., and Than, M. E. (2003) The crystal structure of the proprotein processing proteinase furin explains its stringent specificity. *Nat. Struct. Biol. 10*, 520−526.
(31) Friedrich, R., Fuentes-Prior, P., Ong, E., Coombs, G., Hunter, M., Oehler, R., Pierson, D., Gonzalez, R., Huber, R., Bode, W., and Madison, E. L. (2002) Catalytic Domain Structures of MT-SP1/Matriptase, a Matrix-degrading Transmembrane Serine Proteinase. *J. Biol. Chem. 277*, 2160−2168.
(32) Takeuchi, T., Harris, J. L., Huang, W., Yan, K. W., Coughlin, S. R., and Craik, C. S. (2000) Cellular localization of membrane-type serine protease 1 and identification of protease-activated receptor-2 and single-chain urokinase-type plasminogen activator as substrates. *J. Biol. Chem. 275*, 26333−26342.
(33) Szabo, R., Molinolo, A., List, K., and Bugge, T. H. (2007) Matriptase inhibition by hepatocyte growth factor activator inhibitor-1 is essential for placental development. *Oncogene 26*, 1546−1556.
(34) Benaud, C., Dickson, R. B., and Lin, C. Y. (2001) Regulation of the activity of matriptase on epithelial cell surfaces by a blood-derived factor. *Eur. J. Biochem. 268*, 1439−1447.
(35) Szabo, R., Hobson, J. P., List, K., Molinolo, A., Lin, C. Y., and Bugge, T. H. (2008) Potent inhibition and global co-localization implicate the transmembrane Kunitz-type serine protease inhibitor hepatocyte growth factor activator inhibitor-2 in the regulation of epithelial matriptase activity. *J. Biol. Chem. 283*, 29495−29504.
(36) Miyake, Y., Yasumoto, M., Tsuzuki, S., Fushiki, T., and Inouye, K. (2009) Activation of a Membrane-Bound Serine Protease Matriptase on the Cell Surface. *J. Biochem. 146*, 273−282.
(37) Bugge, T. H., Antalis, T. M., and Wu, Q. (2009) Type II Transmembrane Serine Proteases. *J. Biol. Chem. 284*, 23177−23181.
(38) Thomas, G. (2002) Furin at the cutting edge: From protein traffic to embryogenesis and disease. *Nat. Rev. Mol. Cell Biol. 3*, 753−766.
(39) Harris, M., Firsov, D., Vuagniaux, G., Stutts, M. J., and Rossier, B. C. (2007) A Novel Neutrophil Elastase Inhibitor Prevents Elastase Activation and Surface Cleavage of the Epithelial Sodium Channel Expressed in *Xenopus laevis* Oocytes. *J. Biol. Chem. 282*, 58−64.
(40) Passero, C. J., Mueller, G. M., Rondon-Berrios, H., Tofovic, S. P., Hughey, R. P., and Kleyman, T. R. (2008) Plasmin Activates Epithelial Na^+ Channels by Cleaving the γ Subunit. *J. Biol. Chem. 283*, 36586−36591.
(41) Kishi, K., Yamazaki, K., Yasuda, I., Yahagi, N., Ichinose, M., Tsuchiya, Y., Athauda, S. B. P., Inoue, H., and Takahashi, K. (2001) Characterization of a Membrane-Bound Arginine-Specific Serine Protease from Rat Intestinal Mucosa. *J. Biochem. 130*, 425−430.
(42) Matthews, D. J., Goodman, L. J., Gorman, C. M., and Wells, J. A. (1994) A survey of furin substrate specificity using substrate phage display. *Protein Sci. 3*, 1197−1205.
(43) Shipway, A., Danahay, H., Williams, J. A., Tully, D. C., Backes, B. J., and Harris, J. L. (2004) Biochemical characterization of prostasin, a channel activating protease. *Biochem. Biophys. Res. Commun. 324*, 953−963.
(44) Stockand, J. D., Staruschenko, A., Pochynyuk, O., Booth, R. E., and Silverthorn, D. U. (2008) Insight toward epithelial Na^+ channel mechanism revealed by the acid-sensing ion channel 1 structure. *IUBMB Life 60*, 620−628.
(45) Jasti, J., Furukawa, H., Gonzales, E. B., and Gouaux, E. (2007) Structure of acid-sensing ion channel 1 at 1.9 Å resolution and low pH. *Nature 449*, 316−323.
(46) Henrich, S., Lindberg, I., Bode, W., and Than, M. E. (2005) Proprotein Convertase Models based on the Crystal Structures of Furin and Kexin: Explanation of their Specificity. *J. Mol. Biol. 345*, 211−227.
(47) Diakov, A., Bera, K., Mokrushina, M., Krueger, B., and Korbmacher, C. (2008) Cleavage in the γ-subunit of the epithelial sodium channel (ENaC) plays an important role in the proteolytic activation of near-silent channels. *J. Physiol. 2008*, 154435.
(48) Adebamiro, A., Cheng, Y., Rao, U. S., Danahay, H., and Bridges, R. J. (2007) A Segment of γ-ENaC Mediates Elastase Activation of Na^+ Transport. *J. Gen. Physiol. 130*, 611−629.
(49) Szabo, R., and Bugge, T. H. (2008) Type II transmembrane serine proteases in development and disease. *Int. J. Biochem. Cell Biol. 40* (Directed Issue: Proteasesand Antiproteases in Development, Homeostasis and Disease), 1297−1316.
(50) Lee, M.-S., Tseng, I.-C., Wang, Y., Kiyomiya, K.-i., Johnson, M. D., Dickson, R. B., and Lin, C.-Y. (2007) Autoactivation of matriptase in vitro: Requirement for biomembrane and LDL receptor domain. *Am. J. Physiol. 293*, C95−C105.
(51) Gentzsch, M., Dang, H., Dang, Y., Garcia-Caballero, A., Suchindran, H., Boucher, R. C., and Stutts, M. J. (2010) The cystic fibrosis transmembrane conductance regulator impedes proteolytic stimulation of the epithelial Na^+ channel. *J. Biol. Chem. 285*, 32227−32232.
(52) Gaillard, E. A., Kota, P., Gentzsch, M., Dokholyan, N. V., Stutts, M. J., and Tarran, R. (2010) Regulation of the epithelial Na^+ channel and airway surface liquid volume by serine proteases. *Pfluegers Arch. 460*, 1−17.
(53) Netzel-Arnett, S., Currie, B. M., Szabo, R., Lin, C.-Y., Chen, L.-M., Chai, K. X., Antalis, T. M., Bugge, T. H., and List, K. (2006) Evidence for a Matriptase-Prostasin Proteolytic Cascade Regulating Terminal Epidermal Differentiation. *J. Biol. Chem. 281*, 32941−32945.
(54) Vallet, V., Pfister, C., Loffing, J., and Rossier., B. C. (2002) Cell-Surface Expression of the Channel Activating Protease xCAP-1 is Required for Activation of ENaC in the *Xenopus* Oocyte. *J. Am. Soc. Nephrol. 13*, 588−594.
(55) Svenningsen, P., Uhrenholt, T. R., Palarasah, Y., Skjodt, K., Jensen, B. L., and Skott, O. (2009) Prostasin-dependent activation of epithelial Na^+ channels by low plasmin concentrations. *Am. J. Physiol. 297*, R1733−R1741.